Full Paper: A lower critical solution temperature (LCST) phase transition is reported for blends of the biodegradable polymers poly(D,L-lactide) (PDLA) and poly(ε-caprolactone) (PCL). From light scattering measurements the cloud point curve is determined to have a critical temperature of 86 °C and a critical concentration of mass fraction 36 wt.-% PCL. Optical microscopy of phase-separated films indicates a spinodal morphology at the critical concentration, and droplet phases at off-critical concentrations. After quenching phase separated blends below the melting temperature of PCL (60 °C), the crystallization of PCL is used to positively identify PCL-rich and PDLA-rich phases. When cystallization of PCL follows LCST phase separation, the size, shape, and distribution of crystalline regions can be adjusted by the degree of PCL/PDLA phase separation. Thus, the LCST phase separation offers a novel method to control microphase structure in biodegradable materials. Applications to control of mechanical and physical properties in tissue engineering scaffolds are discussed in light of the results.

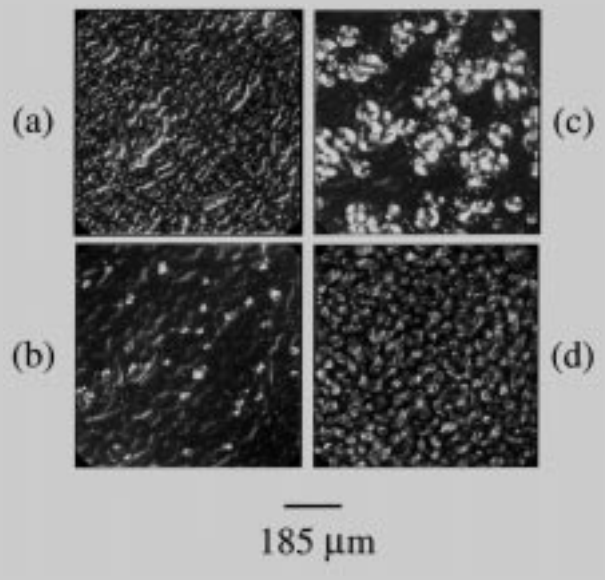

Reflectance mode optical micrographs of a mass fraction 50% PCL/50% PDLA film spun-cast on silicon. (a) 100 °C (two-phase region), 100 min. A droplet phase is observed. (b) After a quench to 30 °C, 3 min, under crossed polars. Bright areas represented growing spherulites of PCL within the continuous PCL rich phase. (c) 30 °C, 5 min. (d) 30 °C, 28 min. Spherulites of PCL impinge upon and do not grow into the PDLA rich droplet phase

LCST phase separation in biodegradable polymer blends: poly(D,L-lactide) and poly(ε-caprolactone)

*J. Carson Meredith, Eric J. Amis**

Polymers Division, National Institute of Standards and Technology, 100 Bureau Dr. Stop 8542, Gaithersburg, MD 20899-8542, U.S.A.
jcm@nist.gov, eric.amis@nist.gov

(Received: September 16, 1999)

Introduction

Although few biological tissues are homogeneous, one-component materials, tissue engineering research to date has focused largely on pure aliphatic polyester scaffolds[1)]. The most popular biodegradable polyesters, homopolymers or copolymers of poly(lactide) (PLA) and poly(glycolide) (PGA), are relatively stiff, brittle, and hard polymers (Tab. 1)[1, 2)]. In contrast biological tissues like cartilage, skin, and tendon are often tough, flexible, or elastic[3)]. The unique mechanical properties of tissue are achieved through a multicomponent extracellular matrix composed of microphase-separated or network structures[3)]. Additionally some tissues contain oriented microstructures that lead to anisotropic mechanical properties[4)].

Tab. 1. Tensile properties of biodegradable polyesters

Polymer	Tensile modulus in GPa	Tensile strength in MPa	Elongation at break in %
PLLA[2)]	3.1	48	2.8
PDLA[24)]	2.2	45	2.6
PGA[2)]	6.3	100	1.5
PCL[25)]	0.15	20.1	400
PLA(85)-*b*-PCL(15)[2)]	0.58	22	500

  1022-1352/2000/0603–0733$17.50+.50/0

Tab. 2. Summary of pure polymer properties (according to the supplier, see text)

Polymer	$\overline{M}_w$ [a)] (Supplier)	T_g [a)] °C	T_m [a)] °C	n (refractive index)	Polydispersity
PDLA	127 000	52.2	–	1.46	1.56
PCL	114 000	–60	60	1.50	1.43

a) $\overline{M}_w$ is the weight average molecular weight, and T_g and T_m are the glass transition and melting temperatures, respectively.

Ideally engineered tissue, consisting of live cells seeded into a synthetic degradable matrix, should have mechanical properties that match the natural tissue it is designed to replace. This is particularly important for load or tension bearing tissues like skin, bone, tendon, cartilage, and muscle, among others. Thus it is necessary to design synthetic degradable scaffolds with properties that more closely match those of native tissues than pure poly(lactides) and poly(glycolides).

An approach often successful with conventional engineered polymers is to strengthen or toughen brittle or stiff materials by incorporating a soft or elastomeric second component into the microstructure. When the softer (lower tensile modulus) component forms a second phase within the more brittle continuous phase, the second phase acts as a stress concentrator, enabling ductile yield mechanisms and preventing brittle fracture[5]. This conventional approach to strengthening polymeric materials may also be applied to biodegradable polymers to develop materials with tissue-like properties. However, application of this method requires detailed knowledge of the phase behavior and microstructure of polymer mixtures. Although numerous studies examine room temperature miscibility of biodegradable blends[6–14], detailed studies of the temperature dependence of phase behavior and microstructure have not been reported for biodegradable polymers.

Poly(ε-caprolactone) (PCL) has a low glass transition temperature of about –60 °C (Tab. 2). PCL is a good candidate for toughening lactide-based polymers due to its lower tensile modulus and higher elongation at break than poly(L-lactide) (PLLA) and PDLA (Tab. 1). For example biodegradable PLA-*b*-PCL block copolymers have been investigated and are found to range from soft to elastic depending on the PCL content (Tab. 1)[15–17]. However, these copolymers are generally more expensive and more difficult to prepare than their homopolymer counterparts. Blending may offer a cost-effective method of achieving a range of mechanical properties, although an ultimate solution may require some combination of both blending and copolymerization. A number of studies have examined the miscibility and mechanical properties of PLA with PCL, several of which are illustrated in Tab. 3[6–8]. Each of these previous studies of PLA/PCL blends examined the miscibility at one temperature, either visually or with differential scanning calorimetry. However the presence of crystalline PLA can obscure detection of liquid-liquid miscibility. Thus, some of the miscibility results are conflicting or incomplete. In addition, rubber toughening of PLA[6, 16] and PLA based urethanes[18] has been achieved with some success by blending with PLA-*b*-PCL copolymers. These previous studies indicate that there is promise in toughening poly-(lactides) by blending with soft or rubbery polymers like PCL or PLA-*b*-PCL. However further progress requires knowledge of the phase behavior, such as the existence and location of the phase boundaries for an upper critical solution temperature (UCST) or a lower critical solution temperature (LCST). It is also necessary to understand the relationship between microstructure developed during phase separation and operating variables like temperature, composition, and time.

In this work thermally induced phase separation in blends of poly(D,L-lactide) (PDLA) and PCL is evaluated as a means to control microstructure in biodegradable polymers. PCL is a crystalline polymer with a relatively low melting temperature near 60 °C. The D,L isomer of lactic acid is chosen to eliminate the added complexity of crystallization that occurs for PLLA. By using light scattering cloud point measurements, we present observation of a LCST phase boundary for this blend pair, previously unreported in the literature. The morphology of the phase-separated blends is characterized with optical microscopy following temperature jumps into the two-phase region. In addition, the distribution of PCL between each phase is identified by quenching below 60 °C after phase separation and monitoring the appearance of crystalline PCL.

Experimental part

Blend preparation

PDLA (Alkermes, Medisorb 100DL, Lot No. 7248-345, $\overline{M}_w$ = 127 000[a, b]) and PCL (Aldrich, Lot No. 07007DN, $\overline{M}_w$ = 114 000) were used as obtained from the supplier. Properties of the pure PDLA and PCL are summarized in Tab. 2. Blends

[a] Certain equipment and instruments or materials are identified in the paper in order to adequately specify the experimental details. Such identification does not imply recommendation by the National Institute of Standards and Technology, nor does it imply the materials are necessarily the best available for the purpose.

[b] According to ISO 31-8, the term "molecular weight" has been replaced by "relative molecular weight" M_r. For clarity, the conventional notation for number average ($\overline{M}_n$) and weight average ($\overline{M}_w$) molecular weight is utilized in the present paper.

were prepared by solvent casting from chloroform (Aldrich, ACS grade). Polymer solutions at a constant mass fraction of 10% were cast in Petri dishes and then dried under vacuum at 60 °C for at least 4 d to remove residual solvent. A range of blend compositions from mass fraction 10% to 60% PCL was prepared in this manner. The resulting films were stored in a vacuum dessicator until experiments were performed.

Cloud point measurement

A laser light scattering apparatus was used to measure cloud points while scanning over temperatures of 80 °C to 130 °C at heating rates of 2.0 °C/min, 1.0 °C/min, and 0.5 °C/min. The detector was positioned at an angle of 20 ° relative to the incident light. A computer interfaced heating stage (Mettler FP-82) controlled the temperature to within 0.1 °C. For the cloud point measurements a 1 cm diameter polymer blend sample was placed in a 0.2 mm thick brass holder and pressed between a glass microscope slide and coverslip. The films were annealed at 75 °C for one hour prior to each temperature scan to melt the PCL. This annealing temperature is in the one phase region for PDLA/PCL but above the 60 °C melting temperature of PCL.

Optical microscopy

An optical microscope (Nikon Optiphot-2) coupled to a CCD camera (Kodak Model ES 1.0) and a vacuum heating stage were used to characterize the morphology of phase separated blends. Because the films were observed to dewet hydrophilic glass surfaces, samples were prepared by spin-casting (Headway Research, Model CB15) on silicon wafers (Semiconductor Processing Company) from chloroform solution (total polymer content mass fraction 10%). The silicon wafers were first acid-cleaned at 100 °C for 1.5 h with a solution of mass fraction 70% H_2SO_4/30% H_2O_2. The hydrophobic silicon was prepared by etching acid-cleaned silicon wafers in a mass fraction 14% aqueous HF solution (J.T. Baker) for 3 min, followed by 5 min in a mass fraction mass fraction 40% NH_4F solution (J. T. Baker). Films were spun at 2000 revolutions per min to yield thicknesses of approximately 20 μm. The films were imaged immediately after spin casting.

Results and discussion

Cloud point determination

Fig. 1 represents scattered intensity versus temperature data for a film containing mass fraction 22% PCL heated at a rate of 2.0 °C/min. These data are typical of all compositions and heating rates. The error bars in Fig. 1 represent the standard deviation in scattered intensity over each 30 s (1 °C) interval of data. As the heating begins, there is a gentle slope downward in scattered intensity as temperature increases, followed by a sharp rise in intensity at about 106 °C. The sharp rise in scattered intensity is characteristic of an LCST phase transition, arising from an increase in concentration fluctuations near the phase

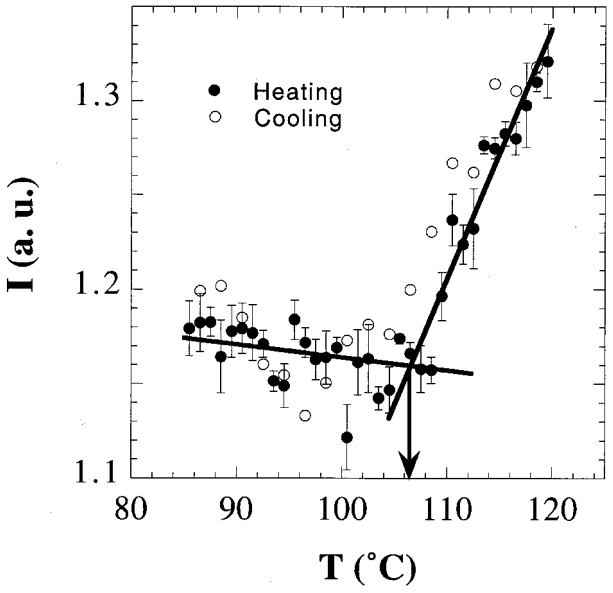

Fig. 1. Scattered intensity versus temperature (°C) for a mass fraction 22% PCL sample heated at 2 °C/min. The error bars are the standard deviation of the scattered intensity within each 1 °C interval

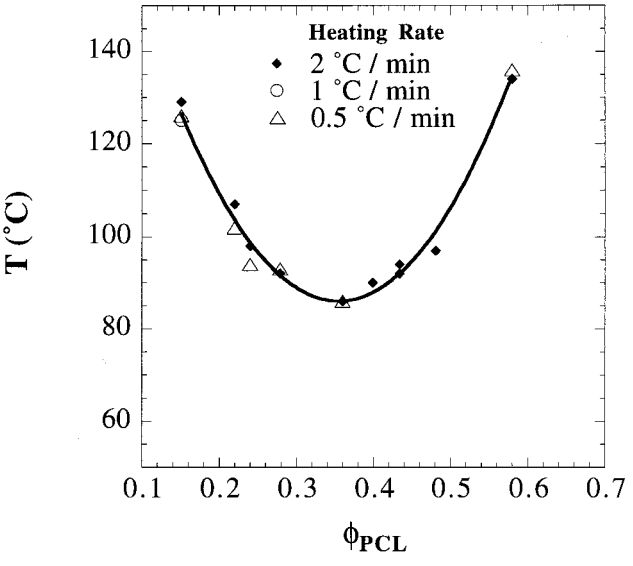

Fig. 2. Cloud point curve for the PDLA/PCL system at three heating rates: 2.0, 1.0, and 0.5 °C/min. The uncertainty in temperature is ±0.5 °C and in composition is ±0.5 mass fraction %

boundary and growth of phase-separated domains[19]. The cloud point is identified as the intersection of lines obtained by a linear least squares fit through the two slopes in the heating data, as shown in Fig. 1. In order to establish that the observed upturn in scattering is a thermodynamic phase transition, it is necessary that the scattering be reversible upon cooling, as is the case in Fig. 1. In fact, the heating and cooling cycle shown in Fig. 1 can be repeated many times, always yielding similar results.

It should be noted that for many of our samples, a hysteresis between the heating and cooling curves was

Tab. 3. Relevant studies of poly(lactide) – poly(ε-caprolactone) blend miscibility

Reference	System[a)]	PCL composition mass fraction in %	Blending method	Miscibility
[6)]	PLLA (365 k, 849 k) PCL (160 k)	20	extrusion, 180–220 °C	immiscible, 25 °C
[7)]	PDLA (325 k) PCL (266 k)	10 to 90	solution cast (CH_2Cl_2)	immiscible, 25 °C for 30 to 70% PCL
[8)]	PLLA (85 k) PCL (15 k)	0 to 50	solution cast ($CHCl_3$)	immiscible, 200 °C

a) Numbers in parentheses are polymer weight average molecular weights before processing. PLLA = poly(L-lactide); PDLA = poly(D,L-lactide).

observed, as is often the case in polymer blends. For all concentrations, the cooling curve levels out to the "baseline" intensity an average of 3 °C lower than the upturn in the heating profile. This hysteresis, which can be minimized by reducing the heating or cooling rate, is indicative of differing kinetics during phase separation (heating) and remixing (cooling). In this paper, we use the upturn of scattered intensity in the *heating* profile as an operational definition of the cloud point.

The small downward slope in scattered intensity during heating below the cloud point temperature in Fig. 1 is most likely due to the temperature dependence of both refractive index and compressibility of the homogeneous polymer blend. For example, it is expected that refractive index, n, should decrease with increasing temperature (due to the density decrease), and that the isothermal compressibility, β, should increase with increasing temperature. For a homogeneous fluid, the scattered intensity, I, is related to n and β according to $I \propto n^2/\beta$[20)]. Thus a decrease in n and increase in β both contribute to a reduction in scattered intensity with increasing temperature in the homogeneous region. In addition, because of the crystalline nature of PCL, we can not rule out the possibility that some homogenization in the regions of melted PCL crystallites may give rise to the gentle downward slope in intensity prior to LCST phase separation. However, we annealed each sample at 75 °C for at least 30 min prior to each heating and cooling cycle, to provide for homogenization after melting of PCL.

The LCST cloud point curve is shown in Fig. 2. Two separate sets of solvent cast blends contribute to the data in Fig. 2. The critical point of the cloud point curve occurs at 86 °C and mass fraction 36% PCL. These results are relatively invariant for heating rates of 2 °C/min, 1 °C/min, and 0.5 °C/min. Despite the invariance to these heating rates, the observed cloud points may still reflect some shift to temperatures higher than the true thermodynamic phase boundary due to kinetic effects. Errors induced by kinetic effects, if any, are likely to be greatest at off-critical concentrations. At off-critical concentrations phase separation initially proceeds via nucleation and growth, and is usually slower than spinodal decomposition that occurs in the critical composition region[21, 22)].

Previous workers have reported both miscible and immiscible solvent cast blends of poly(lactic acid) and PCL at various temperatures, and those most relevant to the present work are described in Tab. 3[6–8)]. The molecular weights of the polymers used in the studies in Tab. 3 are both higher[6, 7)] and lower[8)] than $\overline{M}_w$ in this study. For example, Yang et al. studied solution cast PLLA/PCL blends with $\overline{M}_w$ values of 85 000 (PLLA) and 15 000 (PCL)[8)]. By using DSC and optical microscopy, they report evidence of partial miscibility in the melt at 200 °C for blends containing mass fractions between 10% to 50% PCL. Enhanced crystallization of PLLA in the phase separated blends was attributed to increased PLLA chain mobility due to PCL in PLLA-rich regions[8)]. This PCL-enhanced crystallization of PLLA was independent of the overall PCL concentration. Hence changes in the overall PCL composition did not seem to effect the composition of PCL in the PLLA-rich phase. These observations are consistent with the presence of a phase boundary that intersects 200 °C (such as an LCST curve with critical point below 200 °C). Changes in the overall PCL concentration would thus affect the relative amounts of each phase, but not the distribution of PLLA and PCL between phases. The results of Yang et al. are consistent with the existence of the LCST phase boundary presented in this work, with the LCST shifted to higher temperatures due to the lower molecular weights. The amount of the shift of the LCST is unknown since miscibility was not examined at temperatures other than 200 °C. In addition it is not known how differences between the L-lactide and D,L-lactide isomers will affect the LCST phase boundary (PDLA was used in the present study).

The two other studies in Tab. 3 report phase separation in PLA/PCL blends with $\overline{M}_w$ values higher than those in our study. One study investigated PLLA/PCL blends mixed in an extruder at 180 °C to 220 °C and report immiscibility for a blend containing mass fraction 20% PCL[6)]. This conclusion was based on the observation of a bimodal distribution from size exclusion chromatography (SEC) in chloroform, as well as visual observations. However, it is unclear how the molar mass distribution from SEC in dilute solution relates to blend miscibility. Also, the crystallization of both PCL and PLLA hinders

the unambiguous optical determination of miscibility. Thus these tests of miscibility are not considered definitive.

Another study reports phase separation at 25 °C for PDLA/PCL blends containing mass fractions from 30% to 70% PCL using optical polarized microscopy[7]. The blends were prepared by solvent casting from methylene chloride followed by drying at room temperature. One possible explanation for the apparent immiscibility at 25 °C is a shift in the LCST we observe at 86 °C to near room temperature because of the higher molar mass of their polymers. However, the magnitude of the shift is probably too great (>60 °C) to be caused by the moderate $\bar{M}_w$ difference between that study[7] and ours. Rather the authors suggest that the observed phase separation probably occurs during PCL crystallization at 25 °C as PDLA is expelled from crystalline regions as the spherulites grow[7]. Hence the PCL/PDLA phase separation is a secondary effect caused by PCL crystallization, and does not reflect true immiscibility of PCL and PDLA at 25 °C.

It is important to consider the possibility that high-temperature reactions such as copolymerization or chain scission could alter the blend phase behavior. Transesterification exchange reactions occur in many polyester blends at high temperatures. In our case transesterification would result in the formation of block copolymers of PDLA and PCL. For example, enhanced compatibilization in biodegradable blends of poly(*β*-hydroxybutyrate) and PDLA was attributed to transesterification at temperatures of 190 °C[23]. In Fig. 2 the highest temperature reported is 135 °C where transesterification is not expected to be significant. However, we also observed that PDLA/PCL blends heated to 180 °C for several minutes and then cooled to room temperature did not appear to phase separate at the previously observed LCST when reheated. PDLA-*b*-PCL block copolymers may have formed via transesterification, leading to miscibility and removing the reversible LCST. Evidence of chain scission has also been observed for PLLA/PCL blends processed at temperatures in excess of 180 °C[6].

Optical microscopy

Fig. 3, 4, and 5 show optical micrographs for films of critical and off-critical PCL/PDLA blend compositions. Fig. 3a shows a blend at the critical composition, mass fraction 36% PCL, after 30 min at 75 °C, just below the LCST. The blend is homogeneous with no developed microstructure. Fig. 3b shows the same image area 35 min after a quench to 30 °C under crossed polarizers. The bright areas correspond to crystalline PCL. In Fig. 3c, the critical composition blend is imaged 30 min after a temperature jump to 100 °C, well into the two-phase region shown in Fig. 2. In contrast to Fig. 3a, the micrograph in Fig. 3c indicates a spinodal morphology consistent with

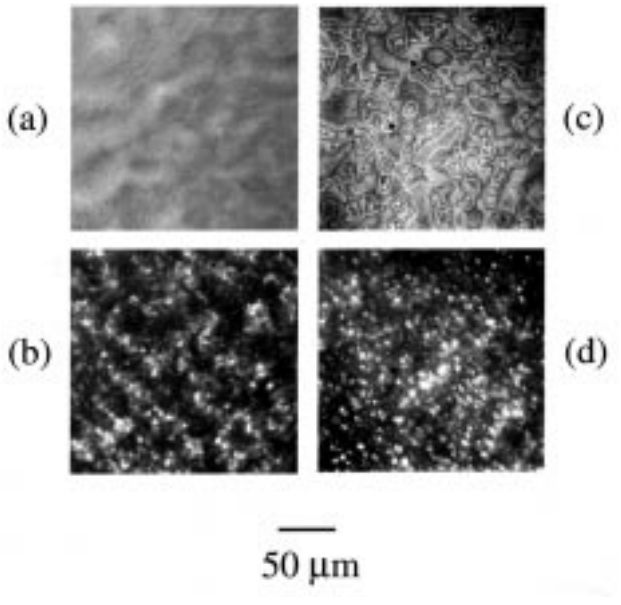

Fig. 3. Reflectance mode optical micrographs of a mass fraction 36% PCL/64% PDLA film spun-cast on silicon. (a) Image taken after 30 min at 75 °C. (b) Image taken 35 min after a quench from 75 °C to 30 °C. (c) 30 min after a temperature jump into the two-phase region at 100 °C, indicating a spinodal microstructure. (d) Crossed polars image taken 30 min after a quench to 30 °C, immediately following 30 min at 100 °C. Bright areas represent ordered crystalline domains of PCL

phase separation at the critical composition. Namely a broken spinodal structure, rich in PCL, is surrounded by a continuous spinodal structure, rich in PDLA. By quenching to 30 °C and observing crystallite growth under crossed polarizers (Fig. 3d), the composition in each phase is identified qualitatively[c]. The bright areas Fig. 3d are attributed to the birefringence of PCL crystallites that are confined to the broken spinodal regions in Fig. 3d, establishing that this phase is rich in PCL. It is difficult to distinguish fine details between the crystallites produced by quenching from 75 °C (Fig. 3b) and 100 °C (Fig. 3d) with optical microscopy. However, in Fig. 3d the crystallites grown from the phase-separated blend (quenched from 100 °C) are clearly associated with the pre-existing LCST microstructure seen in Fig. 3c. The size of the PCL phase ranges from 8 μm (narrow spinodal dimension) to 50 μm (wide dimension). The crystallization of PCL invariably induces a separation between crystalline PCL and the amorphous PDLA/PCL blend, in addition to LCST phase separation in Fig. 3d. However, this crystallization-induced phase separation remains confined to the PCL-rich domains already present due to LCST phase separation.

[c] The quench time was about 3 min. As the phase separated blend cools, PDLA-rich portions become glassy ($T_{g,PDLA}$ = 52 °C) which helps to preserve the preformed spinodal decomposition structure. DSC scans (not shown) indicate that the PDLA glass transition also slows the crystallization rate relative to pure PCL.

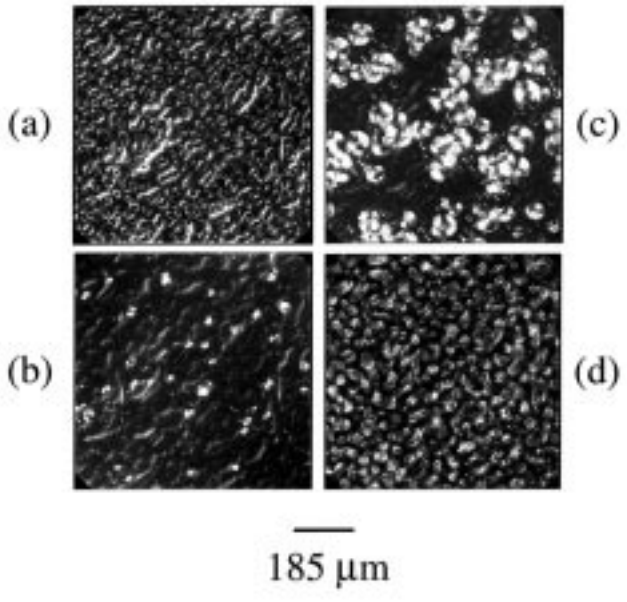

Fig. 4. Reflectance mode optical micrographs of a mass fraction 50% PCL/50% PDLA film spun-cast on silicon. (a) 100 °C (two-phase region), 100 min. A droplet phase is observed. (b) After a quench to 30 °C, 3 min, under crossed polars. Bright areas represented growing spherulites of PCL within the continuous PCL rich phase. (c) 30 °C, 5 min. (d) 30 °C, 28 min. Spherulites of PCL impinge upon and do not grow into the PDLA rich droplet phase

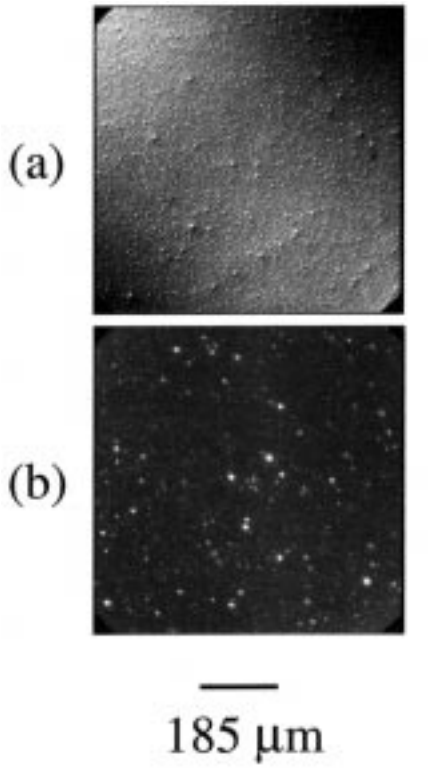

Fig. 5. Reflectance mode optical micrographs of a mass fraction 20% PCL/80% PDLA film spun-cast on silicon. (a) 115 °C (two-phase region), 15 min. (b) 35 min after a quench to 30 °C, under crossed polars

Integration of the bright (PCL-rich phase) and dark areas (PDLA-rich phase) in Fig. 3d (NIH Image software) indicates that 49% of the area is occupied by the PCL phase. This agrees with the cloud point curve in Fig. 2 that shows a critical blend should split into two phases with roughly equal mass at 100 °C (due to the symmetry of the cloud point curve). Here, we have made the assumption that the 2-dimensional surface projection represents the compositions present in the 3-dimensional blend. More quantitative determinations of composition in the surface and bulk of the blend film would require techniques beyond the scope of this work (e.g., XPS, SIMS, FTIR).

Fig. 4a presents an optical micrograph of a mass fraction 50% PCL blend 100 min after a temperature jump to 100 °C. Although the approach to equilibrium is probably not complete at 100 min, it is clear that the blend has separated into droplets, approximately 20 to 30 µm in diameter. Using the cloud point curve as a guide, it is expected that the droplets are rich in PDLA, and the continuous phase is rich in PCL. This is confirmed by quenching the film to 30 °C and observing the appearance of PCL spherulites over time, given in Fig. 4b, 4c, and 4d. Fig. 4b shows that after 3 min PCL spherulites are growing in the continuous phase regions and not in the droplets. Fig. 4c shows that after 5 min some of the spherulites begin to impinge upon one another and upon the PDLA droplets. After 30 min, Fig. 4d, spherulite growth is complete and PCL crystals do not penetrate into the droplet phase. These observations confirm that the droplets are rich in PDLA, in agreement with the cloud point curve (Fig. 3).

Fig. 5a presents an optical micrograph of a mass fraction 20% PCL blend 15 min after a temperature jump into the two-phase region at 115 °C. Many small 1 to 10 µm droplets appear, and are confirmed to be PCL-rich in Fig. 5b after quenching to 30 °C. The bright crystalline regions (under crossed polars) are confined to the small droplets, positively identifying the droplet phase as PCL-rich. Hence the optical micrographs show morphologies and composition distributions that are in agreement with the measured cloud point curve at off-critical and critical compositions.

The microstructural control demonstrated in this paper may lead to rational manipulation of physical, mechanical, and interfacial properties of biomaterials based on PDLA and PCL blends. Mechanical properties, particularly toughness and tensile and impact strength, are critically related to the size of the phase-separated microstructure[5]. By incorporating temperature jumps into the LCST phase boundary, one may successfully blend these two materials with disparate mechanical properties, to achieve improvements in tensile and impact strengths. This level of control could be extremely useful in designing tissue engineering implants to mimic the mechanical

properties of tissue. In addition, the interfacial adhesion at the microphase boundaries is crucial to mechanical strength. A useful way to enhance compatibility at the interface is to add small amounts of PDLA-*b*-PCL block copolymer, or to induce formation of copolymer at the interface by reactive compatibilization.

Conclusions

We report the existence of an LCST phase transition for PCL/PDLA blends. The significance of the LCST phase transition is that phase separation and microstructure can be controlled with both temperature and blend composition. The relationship between PCL/PDLA phase separation followed by PCL crystallization may allow detailed morphological control with programmed temperature jumps (above LCST) and quenches (below the T_m of PCL). For example, the size and distribution of microphase-separated structures can be controlled by adjusting the PCL concentration, temperature, and time inside the LCST two-phase region. Quenching into the one-phase region below the T_m of PCL will lead to PCL crystallization in one or possibly both phases. PCL crystallization should be sensitive to the distribution of PCL between the phases, as set by the LCST phase separation. One may thus achieve control of PDLA and PCL domain sizes as well as PCL crystal ordering by coupling LCST phase separation with crystallization steps. Experiments are planned to investigate the effect of microstructure developed during processing on the mechanical properties. The effect of copolymers on the LCST phase boundary and on mechanical properties will be accessed in future work.

Acknowledgement: J. C. M. gratefully recognizes support of the *NRC/NIST Postdoctoral Research Fellowship*.

[1] J. M. Pachence, J. Kohn, in: "*Principles of Tissue Engineering*", R. Lanza, R. Langer, W. Chick, Ed., Landes Company, Austin, TX, 273 (1997)
[2] E. S. Lipinsky, R. G. Sinclair, *Chem. Eng. Res.* **82**, 26 (1984)
[3] P. A. Davis, S. J. Huang, L. Ambrosio, D. Ronca, L. Nicolais, *J. Mater. Sci. – Mater. Med.* **3**, 359 (1992)
[4] M. S. Sacks, M. C. Jimenez Hamann, S. E. Otano-Lata, T. I. Malinin, *J. Biomech. Eng.* **120**, 541 (1998)
[5] C. B. Bucknall, "*Toughened Plastics*", Applied Science Publishers, Ltd., London (1977)
[6] M. Hiljanen-Vainio, P. Varpomaa, J. Sepala, P. Tormala, *Macromol. Chem. Phys.* **197**, 1503 (1996)
[7] H. Tsuji, Y. Ikada, *J. Appl. Polym. Sci.* **60**, 2367 (1996)
[8] J.-M. Yang, H.-L. Chen, J.-W. You, J. C. Hwang, *Polym. J.* **29**, 657 (1997)
[9] A. J. Domb, *J. Polym. Sci., Part A: Polym. Chem.* **31**, 1973 (1993)
[10] N. Koyama, Y. Doi, *Macromolecules* **29**, 5843 (1996)
[11] M. R. Lostocco, A. Borzacchiello, S. J. Huang, *Macromol. Symp.* **130**, 151 (1998)
[12] G. Rocha, R. Gross, S. McCarthy, *Abstr. Pap. of ACS-POLY* **204**, 184 (1992)
[13] B. J. Tighe, A. J. Amass, M. Yasin, *Macromol. Symp.* **123**, 133 (1997)
[14] L. Zhang, C. Xiong, X. Deng, *J. Appl. Polym. Sci.* **56**, 103 (1995)
[15] M. P. Hiljanen-Vainio, P. A. Orava, J. V. Seppala, *J. Biomed. Mater. Res.* **34**, 39 (1997)
[16] D. W. Grijpma, R. D. A. van Hofslot, H. Super, A. J. Nijenhuis, A. J. Pennings, *Polym. Eng. Sci.* **34**, 1674 (1994)
[17] R. G. Sinclair, Patent # 4045418, Gulf Oil Corporation, USA (1977)
[18] M. Hiljanen-Vainio, J. Kylmae, K. Hiltunen, J. Seppala, *J. Appl. Polym. Sci.* **63**, 1335 (1997)
[19] H. Yang, G. Hadziioannou, R. S. Stein, *J. Polym. Sci. Polym. Phys.* **21**, 159 (1983)
[20] H. R. Allcock, F. W. Lampe, "*Comtemporary Polymer Chemistry*", Prentice Hall, Englewood Cliffs, NJ (1990)
[21] C. C. Han, M. Okada, Y. Muroga, B. J. Bauer, Q. Tran-Cong, *Polym. Eng. Sci.* **26**, 1208 (1986)
[22] T. Sato, C. C. Han, *J. Chem. Phys.* **88**, 2057 (1988)
[23] L. Zhang, C. Xiong, X. Deng, *Polymer* **37**, 235 (1996)
[24] Product Specification for Medisorb 100DL Polymer, Alkermes, Inc., USA
[25] M. Yasin, B. J. Tighe, *Biomaterials* **11**, 133 (1990)